Am J Cancer Res 2026;16(3):1081-1101
www.ajcr.us /ISSN:2156-6976/ajcr0170415

Original Article

hsa-circKLK3-25 promotes epithelial-mesenchymal transition and malignant progression of prostate cancer through the JNK/ERK signaling pathway

Wei Zheng[1], Kebing Yang[1], Cenchao Yao[2], Zhida Wang[3]

[1]Urology and Nephrology Center, Department of Urology, Zhejiang Provincial People's Hospital (Affiliated People's Hospital), Hangzhou Medical College, No. 158, Shangtang Road, Hangzhou 310000, Zhejiang, China; [2]The Second Clinical Medical College, Zhejiang Chinese Medical University, Hangzhou 310053, Zhejiang, China; [3]Postgraduate Training Base Alliance of Zhejiang Provincial People's Hospital, Wenzhou Medical University, Hangzhou 310000, Zhejiang, China

Received November 30, 2025; Accepted March 19, 2026; Epub March 25, 2026; Published March 30, 2026

Abstract: Prostate cancer (PCa) is one of the most common malignant tumors in males. Characterized by an insidious onset, the majority of patients are diagnosed at an advanced stage upon initial presentation. Therefore, it is particularly important to find the potential biomarkers for early diagnosis of PCa. The expression and stability of circKLK3-25 in PCa cells were assessed by qRT-PCR and Actinomycin D testing. Cell Counting Kit-8 assay, EdU staining, scratch-wound assay and transwell experiments were used to make clear the influences of circKLK3-25 on the progression of PCa cells. Target miRNAs of circKLK3-25 was analyzed by bioinformatics. Western blot determined the expressions of proteins associated with the JNK/ERK pathway and epithelial-mesenchymal transition (EMT). Finally, subcutaneous xenograft tumor models were formed in nude mice to uncover the interference of circKLK3-25 with PCa progression *in vivo*. The results showed that circKLK3-25 was significantly highly expressed in PCa cells with good stability. Overexpression circKLK3-25 propelled PCa cells to proliferate, invade, migrate, and EMT process; conversely, silencing circKLK3-25 impaired the malignant biological properties of such cells. Overexpression circKLK3-25 led to upregulation of JNK/ERK signaling pathway-related proteins, while silencing circKLK3-25 lead to the opposite trend. Pathway inhibitors attenuated the pro-oncogenic effects of overexpression of circKLK3-25. circKLK3-25 was a sponge for miR-874-3p, and overexpression of miR-874-3p suppressed the PCa malignant phenotype and EMT. Besides, *in vivo* experiments demonstrated that overexpression circKLK3-25 activated the JNK/ERK signaling pathway and promoted tumor growth, and silencing circKLK3-25 did the opposite. In conclusion, circKLK3-25 is notably overexpressed in PCa cells and promotes PCa malignant progression through activating JNK/ERK signal pathway.

Keywords: Prostate cancer, circKLK3-25, JNK/ERK pathway, proliferation, epithelial-mesenchymal transition

Introduction

Among males, prostate cancer (PCa) stands as a commonly occurring malignant tumor and is the second highest cause of death due to cancer [1-3]. According to worldwide statistics, nearly 1.4 million people were newly affected by PCa and 375,000 people died from this condition in 2020 [4]. The systemic pharmacotherapy based on androgen deprivation therapy (ADT) has long been a standard regimen for treating locally advanced or metastatic PCa [5, 6]. ADT primarily works by reducing the production of androgens in the body to inhibit tumor expansion; whereas, its treatment effectiveness merely lasts 1 to 3 years. Afterward, the condition of most patients may gradually change into castration-resistant prostate cancer (CRPC) [7, 8]. In view of this, identifying reliable molecular markers becomes particularly important for early detection of PCa.

Circular RNA (circRNA) is an endogenous noncoding RNA molecule, extensively presenting in eukaryotes. This molecule does not possess the conventional 5'-cap and 3'-poly tail struc-

https://doi.org/10.62347/GVSL6170

tures but a covalently closed circular structure [9-11]. Generally, circRNAs are generated through a head-to-tail backsplice mechanism. Because circular structures are resistant to degradation by RNase R, circRNAs are more stable than linear RNAs [12, 13]. An increasing body of evidences prove that circRNA, by interaction with DNA, miRNA, lncRNAs, or proteins, regulates the physiological and pathological processes in cells [14, 15]. Significantly, many cancer cells are detected with abnormally expressed circRNAs and this abnormal expression is either oncogenic or tumor-suppressive [16, 17]. However, there is lack of reports on the study of circRNA in PCa cells; most studies on circRNA in PCa are about the circRNA levels in tumor tissues.

Kallikrein-related peptidase 3 (KLK3), a gene for encoding prostate-specific antigen (PSA), is a common molecular marker in prostate clinical practice [18, 19]. KLK3 is highly expressed in the cancer tissues of patients, and its expression is significantly positively correlated with the clinical stage and lymph node metastasis [20]. However, in benign prostatic hyperplasia and prostatitis, PSA is also expressed at an elevated level, which diminishes its specificity as a cancer biomarker [21]. This necessitates the search for more reliable molecular markers. Our group found that PCa cells can highly express a KLK3 gene-derived circRNA molecule (circKLK3-25), and the effect of circKLK3-25 on PCa progression as well as the molecular mechanism has not been reported in studies. The mitogen-activated protein kinase (MAPK) pathway is involved in mediating the biological processes of tumor cells, including metastasis, proliferation, apoptosis, and invasion, while a key part of this pathway is the c-Jun N-terminal kinase (JNK)/extracellular-signal-regulated kinase (ERK) pathway that takes a vital part in the aggressive progression of PCa [22, 23]. PCa patients with lower JNK expression showed higher overall survival [24], whereas activation of the MAPK/ERK pathway promotes epithelial mesenchymal transition (EMT) and thus cell metastasis in PCa cells [25]. However, whether circKLK3-25 regulates the JNK/ERK signaling pathway has not been reported. Therefore, we hypothesize that circKLK3-25 regulates PCa progression by modulating the JNK/ERK pathway. Accordingly, the present study aims to survey circKLK3-25's regulation of the ERK/JNK signal transduction pathway and circKLK3-25's interference with *in vitro/vivo* progression and EMT process of PCa.

Methods and materials

This study was conducted in adherence with ARRIVE guidelines and was approved by the Experimental Animal Ethics Committee of Zhejiang Provincial People's Hospital (Affiliated People's Hospital), Hangzhou Medical College (Ethics clearance number: 2024-183).

Clinical sample collection

Paracancerous normal tissue (n=43) and PCa tissue samples (n=61) were obtained from PCa patients admitted to Zhejiang Provincial People's Hospital (Affiliated People's Hospital) between October 2022 and December 2024. These patients had a preoperative pathological diagnosis confirmed as PCa, none of them had undergone ADT or radiotherapy before surgery, and there were no metastases. The samples were processed by liquid nitrogen flash freezing and stored in an ultra-low temperature refrigerator at -80°C after collection.

Cell culture and transfection

Human RWPE-1 cells from male normal prostate epithelial tissue, RRID CVCL_3791 (https://www.cellosaurus.org/CVCL_3791), purchased from Shanghai Cell Bank of Chinese Academy of Sciences (Stock No.: SCSP-5025) in March, 2023. Human PCa cell lines LNCaP95 cells from male PCa tissue, RRID CVCL_A4DX (https://www.cellosaurus.org/CVCL_A4DX), purchased from BioVector National Typical Culture Collection Inc (Beijing, China, Stock No.: RRID:CVCL_A4DX) in March, 2023. Human PCa cell lines MR49F cells from male PCa tissue, RRID CVCL_RW53 (https://www.cellosaurus.org/CVCL_RW53), purchased from BioVector National Typical Culture Collection Inc (Stock No.: MR49F) in March, 2023. Human PCa cell lines LNCaP cells from male PCa tissue, RRID CVCL_0395 (https://www.cellosaurus.org/CVCL_0395), purchased from Shanghai Cell Bank of Chinese Academy of Sciences (Stock No.: SCSP-5021) in March, 2023. Human PCa cell lines C4-2 cells (LNCaP C4-2) from male PCa tissue, RRID CVCL_4782 (https://www.cellosaurus.org/CVCL_4782), pur-

chased from BioVector National Typical Culture Collection Inc (Stock No.: RRID:CVCL_4782) in March, 2023. Before testing, RWPE-1 cells were immersed in a Keratinocyte-SFM medium (17005042, Gibco, Grand Island, NY, USA) with 1% penicillin and streptomycin (15140122, Gibco) and cultivated at 37°C in an atmosphere with 5% CO_2; PCa cell lines were dipped in a RPMI-1640 medium (11875093, Gibco), which contained 10% fetal bovine serum (A5256701, Gibco) and 1% penicillin and streptomycin, and cultivated under the same condition as RWPE-1 cells. All the cells were sub-cultured once three days; the culture medium was replaced at an interval of two days.

For cell transfection, RiboBio Co., Ltd. (Guangzhou, Guangdong, China) synthesized and provided the circKLK3-25 overexpression plasmid (circKLK3-25) and short hairpin RNA targeting circKLK3-25 (sh-circKLK3-25), miR-874-3p mimics, inhibitor, or their negative controls (Vector and sh-NC, mimics-NC and inhibitor-NC). According to the user manual of Lipofectamine 3000 (L3000150, Invitrogen, Carlsbad, CA, USA), these plasmids were transfected into LNCaP and C4-2 cells.

In signaling pathway exploration, circKLK3-25+SP600125 group cells were first transfected with circKLK3-25 and then treated with JNK inhibitor SP600125 (10 μM, ab120065, Abcam, Cambridge, MA, USA) for 24 h. Cells in the circKLK3-25+U0126 group were first transfected with circKLK3-25 and then treated with the ERK inhibitor U0126 (10 μM, ab120241, Abcam) for 24 h [26].

RNA separation and RNase R treatment

First, we dosed the Trizol reagent (15596026CN, Invitrogen) onto cells LNCaP and C4-2, extracting the total RNA, followed by two treatments with Ambion DNase I (AM2222, Invitrogen) for 30 minutes at 37°C respectively. Next, the RiboMinus™ eukaryote assay kit (A15020, Invitrogen) was used for removing ribosomal RNAs. Further, the method described by Ma *et al*. [27] was taken for reference in treating the purified RNA with RNase R (6U) (RNR07250, Lucigen, Middleton, WI, USA).

Agarose gel electrophoresis and sanger sequencing

A 2% agarose gel solution was prepared using 2 g of agarose (A4718, Sigma-Aldrich, St. Louis, MO, USA). PCR products of RNA were subjected to gel electrophoresis using a 2% agarose gel [28]. Subsequently, RT-PCR amplification of the alternative splicing fragment was performed, followed by Sanger sequencing to validate the authenticity of the alternative splicing site [29].

RNA fluorescence in situ hybridization (FISH)

The specific probe for circKLK3-25 was synthesized by RiboBio Co., Ltd. LNCaP and C4-2 cells were cultured in 12-well plates (with built-in coverslips) and fixed with 4% paraformaldehyde (P1110, Solarbio, Beijing, China) for 15 min. Referring to the instructions of RNA-FISH kit (GF007-50T, Wuhan Servicebio Technology Co., Ltd., Hubei, China), cells were blocked with 200 μL of prehybridization solution at 40°C for 20 min. The probes were diluted with preheated hybridization solution and placed in a hybridizer for overnight incubation at 40°C. After removing the hybridization solution, the cells were washed with PBS, and DAPI working solution (D9542, Sigma-Aldrich) was added dropwise to cover the cells completely, and the cells were stained for 8 min at room temperature and protected from light [30]. The final images were acquired by fluorescence microscope (DM IL LED, Leica, Heidelberg, Germany).

Actinomycin D experiment

At first, cells (LNCaP and C4-2) were inoculated into a 6-well plate, staying overnight. Subsequently, the cells were treated with Actinomycin D (2 mg/L; A4262, Sigma-Aldrich) at 0, 6, 12, 24, and 48 hours, respectively. Then, we collected the cells and conducted qRT-PCR testing to make clear the mRNA expressions of circKLK3-25 and KLK3 [31].

Cell counting kit-8 (CCK-8) assay

Forty-eight hours post transfection, cells (LNCaP and C4-2) were seeded into a 96-well plate at a density of 2.0×10^4 cells/well. After attaching to the well wall, each well of cells were dosed with 100 μL of complete medium that contained 10% of CCK-8 reagent (C0038, Beyotime), followed by 2-hour cell cultivation in a 37°C incubator. After that, the cells were tested using a Varioskan LUX multimode microplate reader manufactured by Thermo Fisher Scientific (Waltham, MA, USA) to acquire the OD_{450} of the cells.

EdU staining

This part was to test the multiplication of cells (LNCaP and C4-2) using the EdU cell proliferation assay kit (E10187; Invitrogen). First, cells (LNCaP and C4-2), 48 hours post transfection, was cultivated in a 100 mg/L EdU-containing medium for 2 hours and then fixed for 30 minutes at an unregulated temperature in a solution with 4% paraformaldehyde. Next, the cells were rinsed two times using PBS solution and later added with a DAPI solution. Subsequently, the mixture container was placed on a shaker working in a setting without light for about 20-minute cultivation. At last, a fluorescence microscope was utilized for observing and photographing the cells.

Scratch-wound assay

Forty-eight hours post transfection, cells (LNCaP and C4-2) were placed into a 6-well plate with pre-drawn horizontal lines. Once the cells adhered to well wall, a 20 μL sterile pipette tip was utilized to gently scratch a line perpendicular to the horizontal line at the bottom of each well. The next was two washes using PBS solution to get rid of cell debris. Subsequently, the cells were administered with a RPMI-1640 medium excluding serum, and cultivated in a 37°C incubator. Later, the healing states of the scratches were observed at 0 and 24 hours separately and the widths of the scratch areas were measured and analyzed using Image J 1.54 h software (Wavne Resband, National Institute of Mental Health, USA).

Transwell experiment

First, 100 μL diluted Matrix-gel (C0383, Beyotime) was added to each transwell chamber (Corning, Tewksbury, MA, USA), staying in an incubator overnight for cell culture. The following day, residual liquid in each chamber was removed, and the remained mixture in the chamber was hydrated with RPMI-1640 medium excluding serum. Afterward, 200 μL of the cell suspension was taken and injected to the upper part of the chamber and a proper amount of 10% fetal bovine serum-containing RPMI-1640 medium to the lower part, staying around 12 hours for cell cultivation. Later, the transwell chamber was taken out, with the matrigel and the cells in the upper part wiped off and cells in the lower part fixed with 4% paraformaldehyde for 30 minutes. Following two washes using PBS solution, the fixed cells were colored for 5 minutes in a solution with 1% of crystal violet (C0121, Beyotime). After two washing steps with PBS, each well of cells was photographed in random fields under a high-magnification microscope and the cells penetrated were counted.

Apoptosis assay

LNCaP and C4-2 cells after different treatments were resuspended in 500 μL Annexin V Binding Buffer (AP107, Multi Sciences, Hangzhou, China). Subsequently, 5 μL of Annexin-V-APC and 5 μL of propidium iodide were added sequentially, mixed thoroughly, and incubated for 15 min in an environment protected from light. Detection was performed with a BD FACSCalibur™ flow cytometer (BD biosciences, San Jose, CA, USA), analyzed by FlowJo software (v10.8, BD biosciences), and apoptosis rates were calculated.

Bioinformatics analysis

The Circbank (https://www.circbank.cn/#/home) database was used to screen circKLK3-25 for potential target-binding microRNAs (microRNAs, miRNAs) and to predict the binding sites of circKLK3-25 and miR-874-3p. In addition, the binding sites of miR-874-3p and ERK were predicted using the ENCORI database (https://rnasysu.com/encori/).

Dual-luciferase reporter assay

The wild-type (WT) and mutant (MUT) dual luciferase reporter plasmids for circKLK3-25 and ERK were synthesized and provided by RiboBio Co., Ltd. WT-circKLK3-25 and mimics, WT-circKLK3-25 and mimics-NC, MUT-circKLK3-25 and mimics, MUT-circKLK3-25 and mimics-NC, WT-ERK and mimics, WT-ERK and mimics-NC, MUT-ERK and mimics, and MUT-ERK and mimics-NC were co-transfected into LNCaP and C4-2 cells using Lipofectamine 3000. Cells were collected after 48 h of incubation and assayed for luciferase activity using the Dual-Lucy Assay Kit (RG027, Beyotime) [32].

Experiment in vivo

BALB/c nude mice were bought from Vitalriver (Beijing, China), housing temperature was 22±

2°C, the relative humidity was 50%-60%, and a light/dark cycle of 12 h. Regularly sanitizes facilities, like food containers, cage boxes, and water bottles. After 1 week of acclimatization, the nude mice were split into 4 groups in a random manner, with 4 mice in each group. C4-2 cells, following transfection with sh-circKLK3-25, sh-NC, circKLK3-25 or Vector were vaccinated into the right bellies of the mice (2×10^7 cells/mice). After that, the mice's survival states were monitored; the lengths and widths of subcutaneous tumors formed in the mice were measured every week using a caliper. On day 28, pentobarbital sodium (40 mg/kg) were injected into the veins of the mice to euthanize them, followed by tumor separation and photographing for record.

QRT-PCR

Total RNA was extracted from cells and tumor tissues using Trizol reagent and treated with DNase I to eliminate genomic DNA contamination. RNA concentration and purity were detected by NanoDrop microspectrophotometer (Thermo Fisher Scientific), and RNA integrity was verified by agarose gel electrophoresis. Then, AMV reverse transcriptase (2621, TAKARA, Tokyo, Japan) as well as random hexamer primers (N8080127, Invitrogen) were used to synthesize cDNAs, PCR was then performed using divergent primers specific to the circKLK3-25 reverse splice junction. The specificity of the primers was confirmed by Sanger sequencing of the amplified fragments and melting curve analysis. The target genes were then PCR amplified using TB Green FAST qPCR (CN830S, TAKARA) and by a PRISM 7300 RT-PCR system (ABI, Carlsbad, CA, USA). The stability of the reference gene GAPDH in this study was validated via the geNorm algorithm (M value <0.5). The expression levels of all target genes, including circKLK3-25, were normalized to GAPDH, and the relative expression levels of target genes were calculated using the $2^{-\Delta\Delta Ct}$ method. The primer sequences used in this study are as follows: GAPDH: F: 5'-ATGTTGCAACCGGGAAGGAA-3', R: 5'-CGCCCAATACGACCAAATCAGA-3'; KLK3: F: 5'-CTCACGGATGCTGTGAAGGT-3', R: 5'-TAGGGATGACTCACCGAGCA-3'; circKLK3-25 (divergent primer): F: 5'-GCCCACTTGTCTGTAATGGTG-3', R: 5'-TCAGGATGAAACAGGCTGTGC-3'; E-cadherin: F: 5'-TCCAACAGGGACAAAGAAACAA-3', R: 5'-TGACACGGCATGAGAATAGAGG-3'; Vimentin: F: 5'-AGGCAAAGCAGGAGTCCACTGA-3', R: 5'-ATCTGGCGTTCCAGGGACTCAT-3'.

Immunohistochemistry

The tumor tissues were treated with 4% paraformaldehyde for fixation for 24 h. Sections (4 μm) were dehydrated with graded ethanol (100%, 95%, 75% and 50%), paraffin-embedded, deparaffinized with xylene (X821391, Macklin, Shanghai, China) and hydrated with graded ethanol. Then, the sections were placed in 0.1 mol/L citric acid solution (pH=6) and microwaved to repair the antigen. Incubated in 3% H_2O_2 solution for half an hour and rinsed well with PBS. The tissue was covered evenly with 5% bovine serum albumin (BSA, A801320, Macklin) and closed for half an hour. Added dropwise antibody against Ki-67 (MA5-14520, 1:100, Invitrogen) and left to incubate for 1.5 h at 37°C; after being rinsed, the sections were put in a solution with secondary antibody goat anti-rabbit IgG (G-21234, 1:500, Invitrogen), staying for 2 hours of cultivation. The color was developed with DAB (P0203, Beyotime), and when the color development reached the expected effect, distilled water was used to terminate the color development. After hematoxylin (H3136, Sigma-Aldrich) counterstaining, distilled water washing, and neutral balsam (C0173, Beyotime) sealing, the sections were observed through a fluorescence microscope.

Immunofluorescence

Paraffin sections of tumor tissues were placed in PBS and rinsed three times for 5 min each, and exposed to 0.3% Triton X-100 (T824275, Macklin) for 10 min. The sections were shaken dry, 5% BSA was added dropwise, and closed for 1 h at room temperature. The blocking solution was shaken off, and the samples were incubated overnight at 4°C with primary antibody E-cadherin (ab40772, 1:100, Abcam) or Vimentin (ab92547, 1:50, Abcam). After that, the sections were rinsed with PBS and exposed to FITC-labeled goat anti-rabbit secondary antibody (F-2765, 1:500, Invitrogen) for 1 h. Sections were sealed with Antifade Mounting Medium with DAPI (P0131, Beyotime), avoiding air bubbles during the sealing process, then observed under a microscope.

TUNEL staining

Tumor tissue paraffin sections were routinely dewaxed and hydrated, and DNase-free proteinase K (20 μg/mL, ST532, Beyotime) was added dropwise to cover the tissue sections, and the reaction was carried out at 37°C for 15 min. Then TUNEL assay solution (C1086, Beyotime) was added dropwise and incubated for 60 min in an environment protected from light. Then DAPI staining solution was added to cover the tissues, and the staining was protected from light for 10 min, then observed and photographed by fluorescence microscope.

Western blot

RIPA lysis buffer (R917927, Macklin) was mixed well with cells and tumor tissues, and the samples were lysed sufficiently to extract proteins. After lysis was completed, the protein levels of the obtained samples were assessed through the BCA Protein Assay Kit (B917925, Macklin). Next, the extracted protein supernatant was mixed with SDS-PAGE protein upsampling buffer, separated by SDS-PAGE electrophoresis, then transferred to PVDF membranes (88518, Invitrogen) and closed with 5% BSA for 2 h [33]. Subsequently, in a temperature setting of 4°C, the membrane was exposed to primary antibody against p-JNK (44-682G, 1:1000, Invitrogen), JNK (44-690G, 1:1000, Invitrogen), p-ERK (44-680G, 1:1000, Invitrogen), ERK (MA5-15134, 1:1000, Invitrogen), N-cadherin (ab76011, 1:5000, Abcam), E-cadherin (ab40772, 1:1000, Abcam), Snail (ab216347, 1:1000, Abcam), SLUG (PA5-20289, 1:1000, Invitrogen), Twist1 (ab323385, 1:1000, Abcam), Zinc Finger E-Box Binding Homeobox 1 (ZEB1, ab203829, 1:500, Abcam), or Vimentin (ab92547, 1:2000, Abcam) for one night. On the next day, after three rinsing steps, the membrane was immersed in a solution of goat anti-rabbit secondary antibody IgG (ab205718, 1:2000, Abcam) for 2 h. Followed by, tDeveloping solution (P0018S, Beyotime) was prepared and dropped evenly on the membrane, then scanned with a gel imaging system (iBright CL1500, Invitrogen). In the end, the images were processed by the Image J software, where the GAPDH (MA5-35235, 1:50000, Invitrogen) was used for internal reference.

Statistical analysis

For the minimum, three repetitions were conducted for each experiment, with results recorded as mean ± standard deviation. The statistical analysis of all data was utilized using SPSS version 26.0 (IBM SPSS Statistics 26), while Graphpad Prism 9 software was utilized to drawn the statistical graphs. Statistical analyses were performed using nonparametric tests: the Kruskal-Wallis test for multiple comparisons, followed by Dunn's post-hoc test for two comparisons between groups; and the Mann-Whitney U test for two-group comparisons. For data from consecutive time points, the assumption of sphericity of the data was verified by Mauchly's test: if sphericity was met ($P>0.05$), a repeated-measures ANOVA was used; if it was not met ($P<0.05$), the Greenhouse-Geisser correction coefficients were applied to ensure the reliability of the statistical results. $P<0.05$ denotes significant differences.

Results

Presence of circKLK3-25 in PCa cells

To know about whether the KLK3 gene encodes the circRNA, we designed two sets of reverse primers with linear mRNA sequences and performed RT-PCR amplification using cDNA from LNCaP cells. Two PCR products were examined through DNA electrophoresis, purified using agarose gel, and then cloned into PCR4 TOPO vectors separately. The Sanger sequencing consequences confirmed that the products of both sets of primers pointed to the same circular shear site, indicating that both products were derived from circKLK3-25 (**Figure 1A**, **1B**). **Figure 1C** illustrates the loop shear site of the linear mRNA. Moreover, we again designed multiple sets of reverse primers and performed RT-PCR on cDNA extracted from reverse transcription of LNCaP cells, all of which yielded the target product, confirming the presence of circKLK3-25 molecule (**Figure 1D**).

Elevated expression of circKLK3-25 in PCa cells

The expression of circKLK3-25 in PCa patient samples was detected by qRT-PCR. The results showed that the expression level of circKLK3-25 in PCa tissue was significantly increased

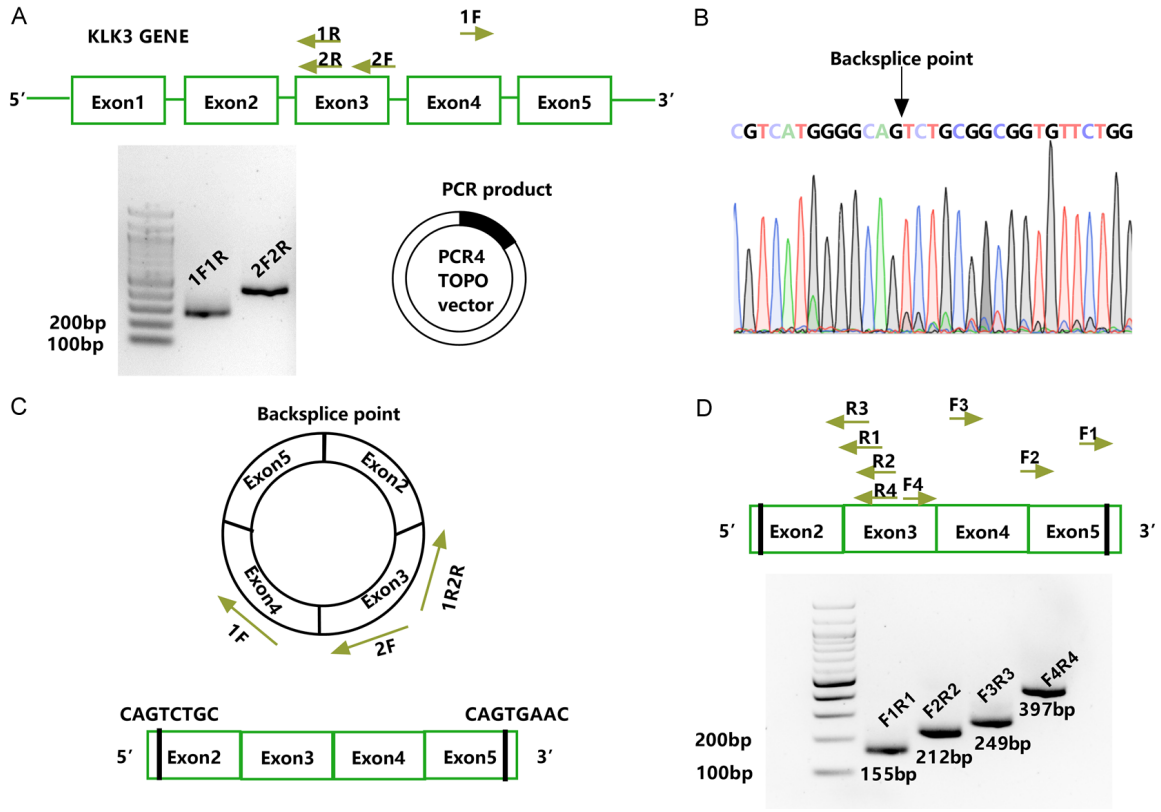

Figure 1. Verification of the expressions of circKLK3-25 in PCa cells. A. Two sets of reverse primers were devised and utilized for RT-PCR amplification of cDNAs obtained from LNCaP cells. B. The products of both sets of primers pointed to the same circular shear site (circKLK3-25). C. Loop shear sites of linear mRNAs. D. RT-PCR was performed on cDNA from LNCaP cells, confirming the presence of circKLK3-25 in PCa cells.

compared with adjacent normal tissue (**Figure 2A**). The expressions of circKLK3-25 in RWPE-1 cells and PCa cell lines (LNCaP95, MR49F, LNCaP, and C4-2) were detected through qRT-PCR experiments. The results reveal that PCa cell lines had circKLK3-25 levels evidently superior to RWPE-1 cells; among the PCa cell lines, C4-2 cells possessed the highest circKLK3-25 level, followed by LNCaP cells (**Figure 2B**). Hence, LNCaP and C4-2 cells were utilized for the follow-up experiments. What's more, circKLK3-25 was insusceptible to RNase R, displaying a higher stability than linear KLK3 mRNA (**Figure 2C**, **2D**). The actinomycin D experimental results also suggest that circKLK3-25 is highly stable, evidenced by the half-lives of the circKLK3-25 transcript (exceeding 48 hours) and KLK3 transcript (merely about 18 hours) (**Figure 2E**, **2F**). Furthermore, we employed RNA-FISH technology to examine the subcellular localization of circKLK3-25. The results indicated that circKLK3-25 was enriched in the cytoplasm of PCa cells (**Figure 2G**).

Overexpression circKLK3-25 promotes PCa cell proliferation, migration, and invasion and EMT

To make clear the role of circKLK3-25 in the aggressive behavior of PCa cells, we had cells LNCaP and C4-2 transfected with circKLK3-25 and tested by means of qRT-PCR to know about the efficiency of excessive circKLK3-25. As a result, the cells transfected with circKLK3-25 obtained apparently heightened circKLK3-25 levels than those transfected with Vector. This indicates that the transfection efficiency met the experimental requirements (**Figure 3A**). Through CCK-8 experiments and EdU staining, excessive circKLK3-25 was found to be greatly helpful to the proliferation of cells LNCaP and C4-2 (**Figure 3B-D**). Following the excessive expression of circKLK3-25, these cells also acquired higher abilities to migrate as confirmed by scratch-healing experiments (**Figure 3E**) and to penetrate as evidenced by transwell experiments (**Figure 3F**). Flow cytometry

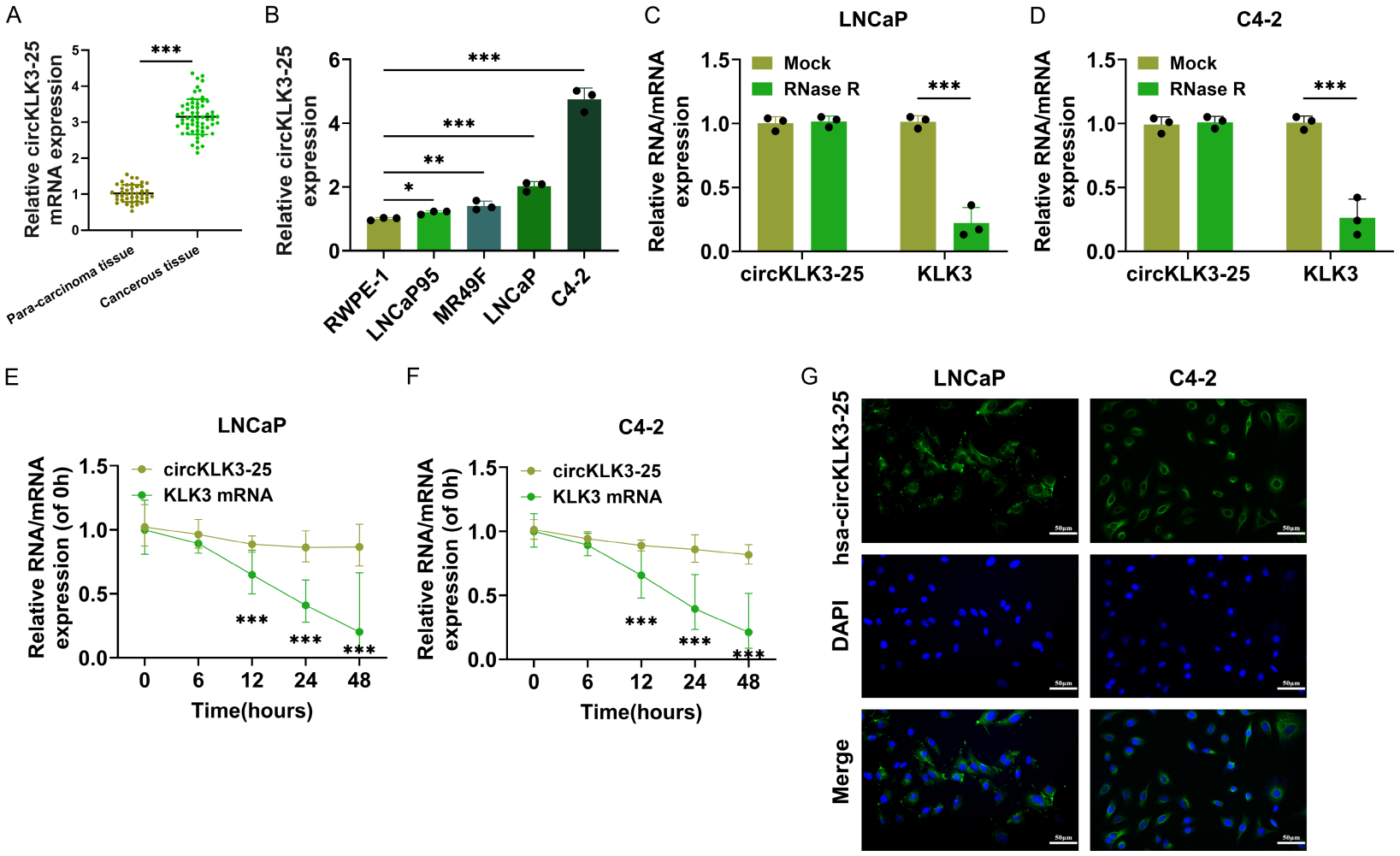

Figure 2. Elevated expression of circKLK3-25 in PCa cells. A. qRT-PCR detection of circKLK3-25 expression in cancer tissues (n=61) and paracancerous tissues (n=43) of PCa patients. B. qRT-PCR detected circKLK3-25 expression in RWPE-1 cells and PCa cell lines (LNCaP95, MR49F, LNCaP, and C4-2). C, D. Stability of circKLK3-25 and linear KLK3 mRNA expression in PCa cells detected by qRT-PCR. E, F. Actinomycin D assay for the detection of half-life and stability of circKLK3-25. G. RNA-FISH detection of circKLK3-25 enrichment in PCa cells. n=3. *P<0.05, **P<0.01, ***P<0.001.

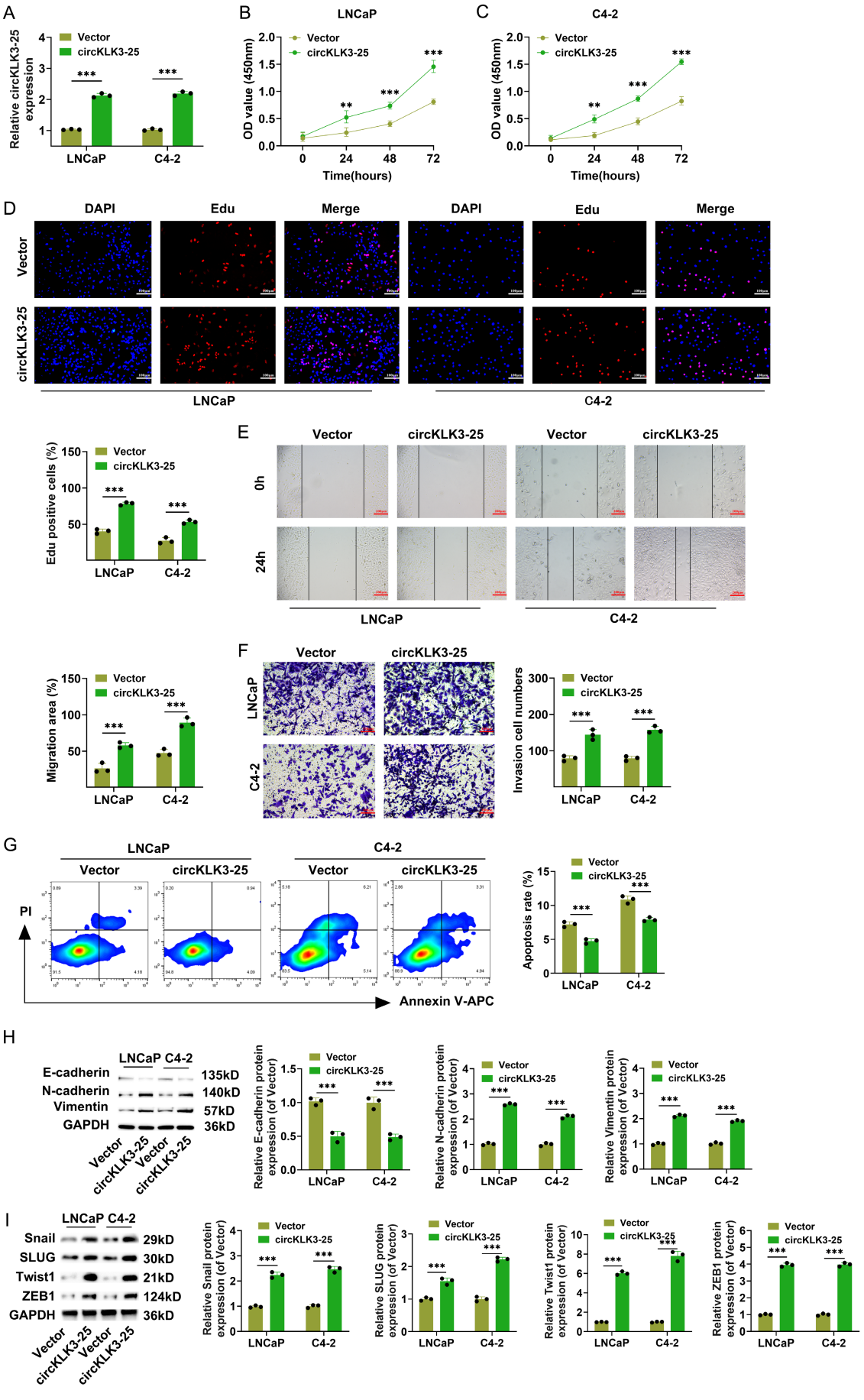
A
Relative circKLK3-25 expression
Vector
circKLK3-25
LNCaP
C4-2
B
LNCaP
OD value (450nm)
Time(hours)
C
C4-2
D
DAPI
Edu
Merge
Vector
circKLK3-25
LNCaP
C4-2
Edu positive cells (%)
E
0h
24h
Migration area (%)
F
Invasion cell numbers
G
PI
Annexin V-APC
Apoptosis rate (%)
H
E-cadherin
N-cadherin
Vimentin
GAPDH
135kD
140kD
57kD
36kD
Relative E-cadherin protein expression (of Vector)
Relative N-cadherin protein expression (of Vector)
Relative Vimentin protein expression (of Vector)
I
Snail
SLUG
Twist1
ZEB1
29kD
30kD
21kD
124kD
Relative Snail protein expression (of Vector)
Relative SLUG protein expression (of Vector)
Relative Twist1 protein expression (of Vector)
Relative ZEB1 protein expression (of Vector)

Figure 3. Overexpression of circKLK3-25 promotes proliferation, migration, invasion and EMT in PCa cells. A. qRT-PCR detection of circKLK3-25 expression level in PCa cells after transfection with circKLK3-25. B, C. CCK-8 assay to detect the viability of LNCaP and C4-2 cells after overexpression of circKLK3-25. D. EdU staining determined cell proliferation after overexpression of circKLK3-25 (20×, 100 μm). E. Scratch-wound assay detected cell migration after transfection with circKLK3-25 (10×, 200 μm). F. Transwell assay to assess cell invasion after overexpression of circKLK3-25 (20×, 100 μm). G. Flow cytometry to detect apoptosis rate. H, I. Western blot detect E-cadherin, N-cadherin, Vimentin, Snail, SLUG, Twist1, and ZEB1 levels in LNCaP and C4-2 cells after overexpression of circKLK3-25. n=3. $^{**}P<0.01$, $^{***}P<0.001$.

assay showed that the apoptosis rate of LNCaP and C4-2 cells was significantly reduced after overexpression of circKLK3-25 (**Figure 3G**). Additionally, Western blot findings showed that overexpression circKLK3-25 caused a significant decline in E-cadherin level and a significant rise in N-cadherin, Vimentin, Snail, SLUG, Twist1, and ZEB1 levels in LNCaP and C4-2 cells (**Figure 3H**, **3I**). To sum up, circKLK3-25 overexpression promotes malignant biological behavior, inhibits apoptosis, and promotes EMT in PCa cells.

Silencing circKLK3-25 suppresses PCa cell proliferation, migration and invasion and EMT

Subsequently, sh-circKLK3-25 was transfected into cells LNCaP and C4-2. In consequence, circKLK3-25 in these cells was leveled down to a large extent as demonstrated by qRT-PCR experiments (**Figure 4A**). After circKLK3-25 got silenced, these cells became weakened in proliferation as displayed in the results of EdU staining and CCK-8 experiments (**Figure 4B-D**), in migration as found through scratch-healing experiments (**Figure 4E**), as well as in penetration as detected through transwell experiments (**Figure 4F**). In addition, the apoptosis rate of LNCaP and C4-2 cells was significantly elevated after silencing circKLK3-25 (**Figure 4G**). Silencing circKLK3-25 also caused markedly higher E-cadherin level and markedly lower N-cadherin, Vimentin, Snail, SLUG, Twist1, and ZEB1 levels in LNCaP and C4-2 cells (**Figure 4H**, **4I**). These findings affirm that silencing circKLK3-25 inhibits the malignant biological behavior of PCa cells.

circKLK3-25 regulates the JNK/ERK signaling pathway

To find the way circKLK3-25 modulates the worsening of PCa, we tested the expressions of p-JNK, JNK, p-ERK, and ERK (proteins of the JNK/ERK signal transduction pathway) by western blot. Consequently, LNCaP and C4-2 cells exhibited amplification in the expressions of the said four proteins following the heightening of circKLK3-25, but attenuation in these expressions following the silencing of circKLK3-25 (**Figure 5A-E**). This phenomenon proves the competence of circKLK3-25 to modulate the JNK/ERK signal transduction pathway. Besides, the JNK inhibitor SP600125 (10 μM) and the ERK inhibitor U0126 (10 μM) attenuated the activation effect of over-expressed circKLK3-25 on the JNK/ERK pathway (**Figure 5F-H**). This further affirms that circKLK3-25 can regulate the JNK/ERK pathway.

circKLK3-25 promotes malignant biological progression of PCa cells through the JNK/ERK signaling pathway

As demonstrated by CCK-8 experiments and EdU staining, excessive circKLK3-25 can strengthen the ability of cells LNCaP and C4-2 to multiply. SP600125 and U0126 reduced the promoting effect of circKLK3-25 overexpression on the malignant biological behavior of PCa cells. SP600125 and U0126 resulted in reduced PCa cell viability (**Figure 6A**, **6B**), decreased EdU positivity (**Figure 6C**), and significantly reduced cell migration and invasion (**Figure 6D**, **6E**). Moreover, SP600125 and U0126 treatments increased the apoptosis rate of LNCaP and C4-2 cells (**Figure 6F**). SP600125 and U0126 reduced the promotion of EMT in PCa cells by overexpression circKLK3-25, resulting in notably higher E-cadherin level and notably lower N-cadherin, Vimentin, Snail, SLUG, Twist1, and ZEB1 levels (**Figure 6G**, **6H**). The above results indicate that SP600125 or U0126 can partially attenuate the promoting effect of circKLK3-25 overexpression on the malignant biological behavior of PCa cells, suggesting that circKLK3-25 exerts its pro-carcinogenic effect by regulating the JNK/ERK pathway.

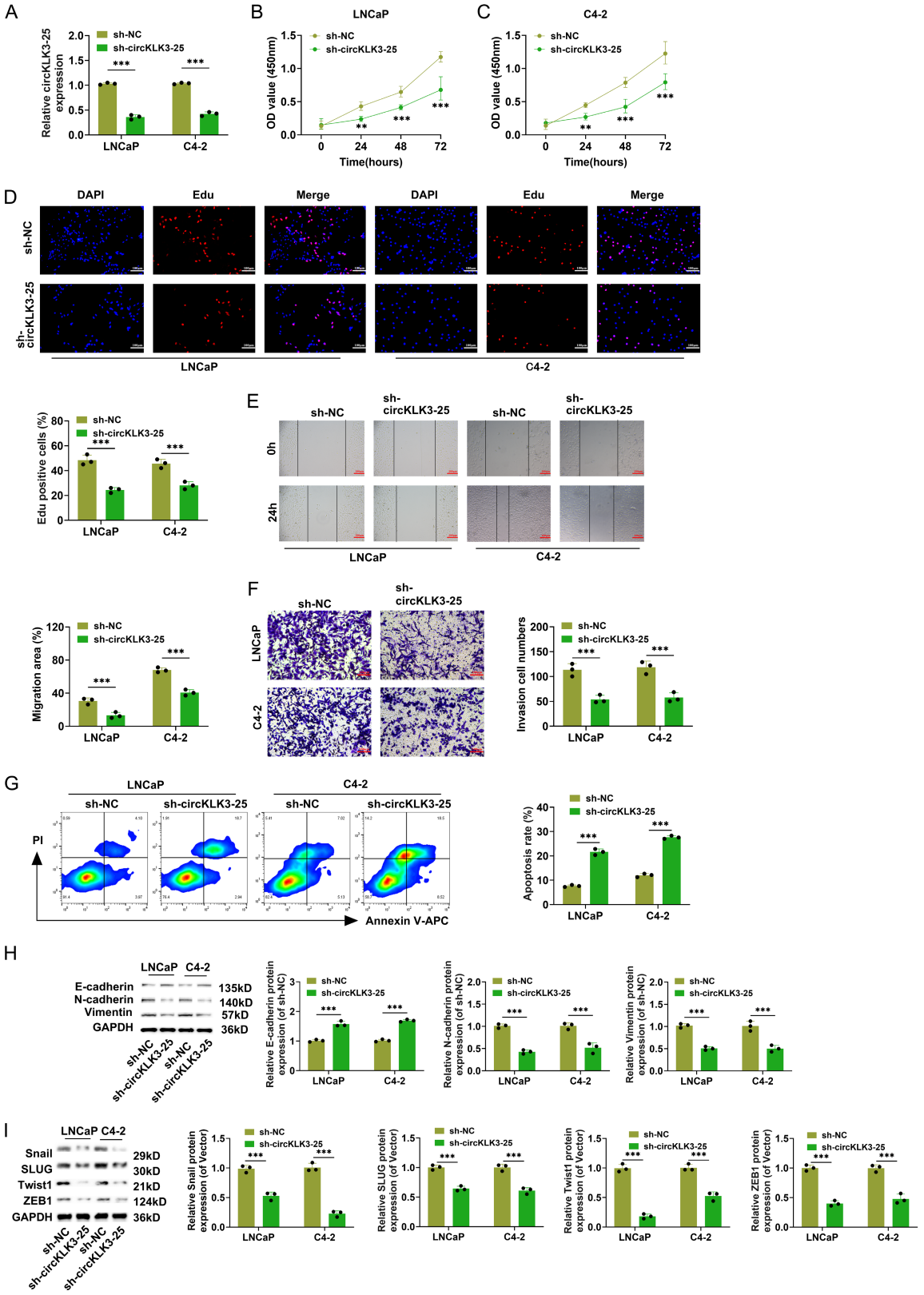

Figure 4. Silencing circKLK3-25 suppresses proliferation, migration, invasion and EMT in PCa cells. A. qRT-PCR detection of circKLK3-25 expression level in PCa cells after transfection of sh-circKLK3-25. B, C. CCK-8 assay to detect the viability of LNCaP and C4-2 cells after silencing circKLK3-25. D. EdU staining results determined cell

proliferation after silencing circKLK3-25 (20×, 100 μm). E. Scratch-wound assay detected cell migration ability after transfection of sh-circKLK3-25 (10×, 200 μm). F. Transwell assay confirmed determined cell invasion capacity after silencing circKLK3-25 (20×, 100 μm). G. Flow cytometry to detect apoptosis rate. H, I. The E-cadherin, N-cadherin, Vimentin, Snail, SLUG, Twist1, and ZEB1 levels in LNCaP and C4-2 cells as examined by Western blot. n=3. ***P*<0.01, ****P*<0.001.

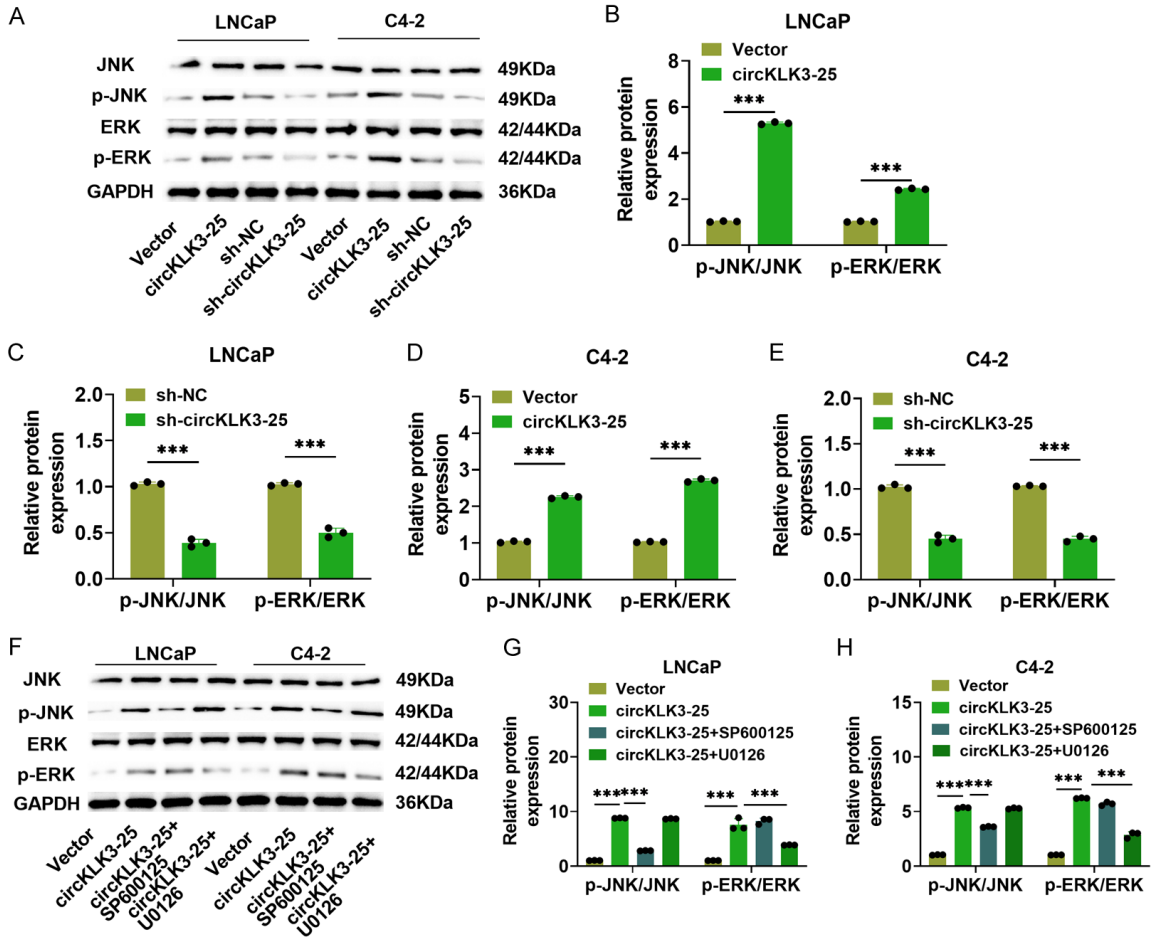

Figure 5. circKLK3-25 regulates the JNK/ERK signaling pathway. A-E. Western blot measured p-JNK/JNK and p-ERK/ERK levels in LNCaP and C4-2 cells after overexpression of circKLK3-25 or silencing circKLK3-25. F-H. Western blot measured p-JNK/JNK and p-ERK/ERK levels in LNCaP and C4-2 cells after the JNK inhibitor SP600125 or the ERK inhibitor U0126 treatment. n=3. ****P*<0.001.

circKLK3-25 acts as sponge for miR-874-3p, and overexpression of miR-874-3p inhibits the PCa malignant phenotype and EMT

The target binding site of circKLK3-25 to miR-874-3p predicted by the Circbank database was shown in **Figure 7A**. Next, we transfected miR-874-3p mimics, mimics-NC, inhibitor, or inhibitor-NC in LNCaP and C4-2 cells. Transfection of mimics significantly elevated miR-874-3p expression in cells, whereas transfection of inhibitor significantly downregulated miR-874-3p levels (**Figure 7B**). Dual luciferase assay showed that overexpression of miR-874-3p significantly inhibited the luciferase activity of WT-circKLK3-25, whereas it had no significant effect on MUT-circKLK3-25, confirming that miR-874-3p could bind to circKLK3-25 (**Figure 7C**, **7D**). In addition, overexpression of circKLK3-25 decreased miR-874-3p expression, whereas silencing of circKLK3-25 resulted in elevated miR-874-3p expression (**Figure 7E**). Silencing of miR-874-3p significantly elevated p-JNK/JNK, p-ERK/ERK in LNCaP and

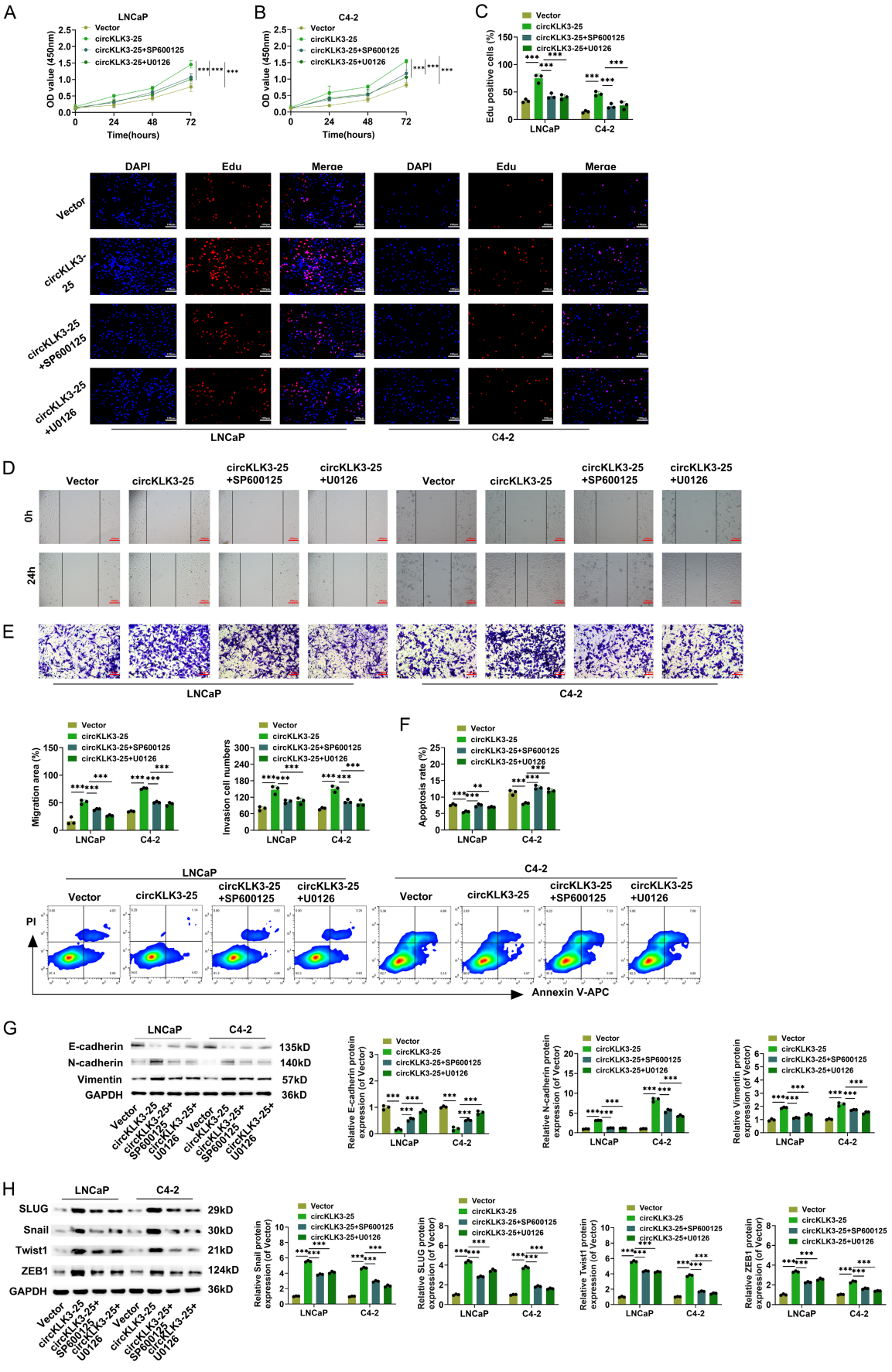
A
LNCaP
B
C4-2
Vector
circKLK3-25
circKLK3-25+SP600125
circKLK3-25+U0126
OD value (450nm)
Time(hours)
C
Edu positive cells (%)
DAPI
Edu
Merge
LNCaP
C4-2
D
0h
24h
E
Migration area (%)
Invasion cell numbers
F
Apoptosis rate (%)
PI
Annexin V-APC
G
E-cadherin
N-cadherin
Vimentin
GAPDH
135kD
140kD
57kD
36kD
Relative E-cadherin protein expression (of Vector)
Relative N-cadherin protein expression (of Vector)
Relative Vimentin protein expression (of Vector)
H
SLUG
Snail
Twist1
ZEB1
GAPDH
29kD
30kD
21kD
124kD
36kD
Relative Snail protein expression (of Vector)
Relative SLUG protein expression (of Vector)
Relative Twist1 protein expression (of Vector)
Relative ZEB1 protein expression (of Vector)

Figure 6. circKLK3-25 promotes PCa cell proliferation, migration, invasion and EMT via the JNK/ERK signaling pathway. A, B. CCK-8 assay measured the impact of SP600125 or U0126 treatment on LNCaP and C4-2 cell viability. C. EdU staining detected cell proliferation after SP600125 or U0126 treatment (20×, 100 μm). D. Scratch-wound assay measured cell migration after SP600125 and U0126 treatment (10×, 200 μm). E. Transwell assay detected cell invasion after SP600125 and U0126 treatment (20×, 100 μm). F. Flow cytometry to detect apoptosis rate. G, H. Western blot measured E-cadherin, N-cadherin, Snail, SLUG, Twist1, ZEB1, and Vimentin expression levels in LNCaP and C4-2 cells. n=3. ***P<0.001.

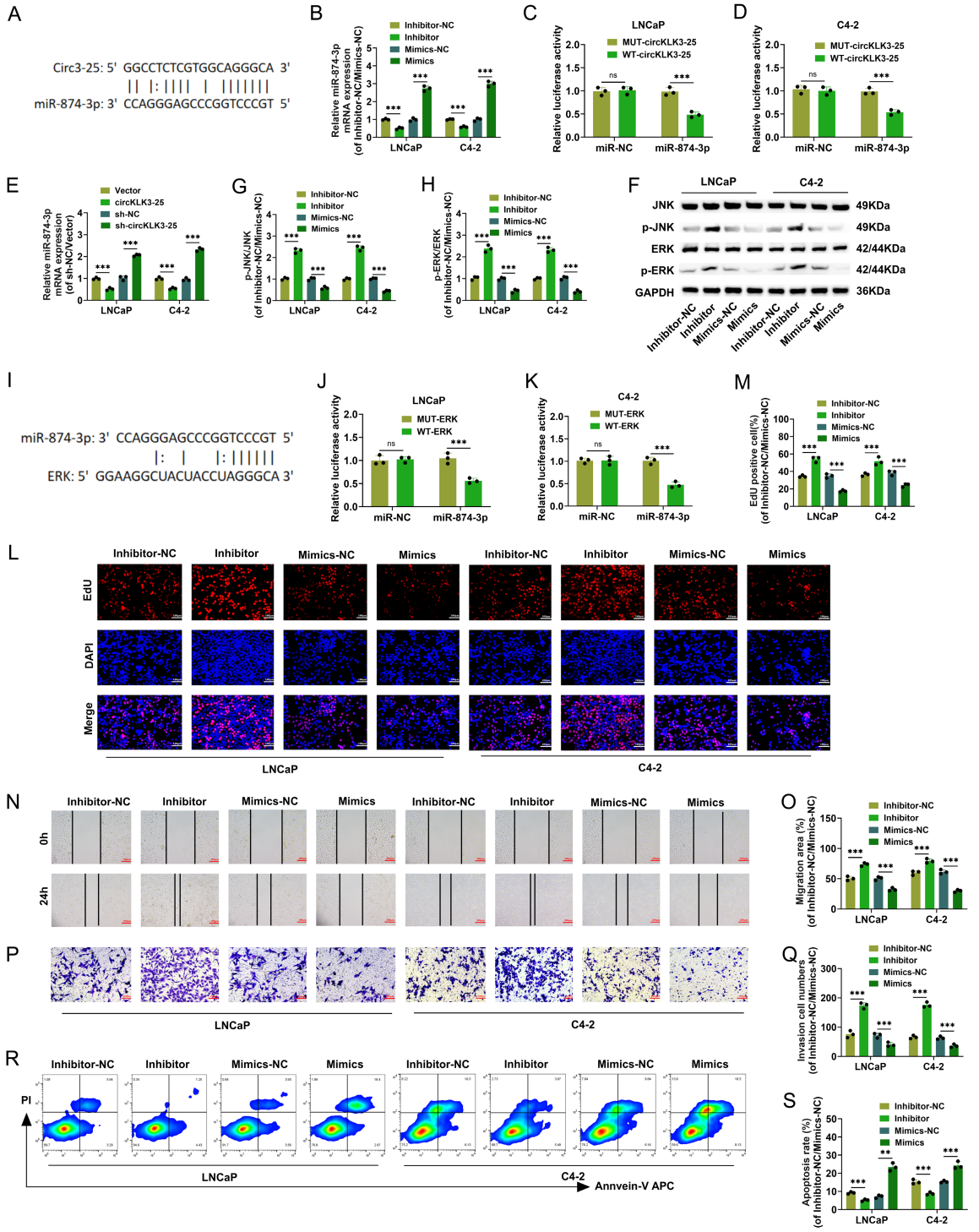

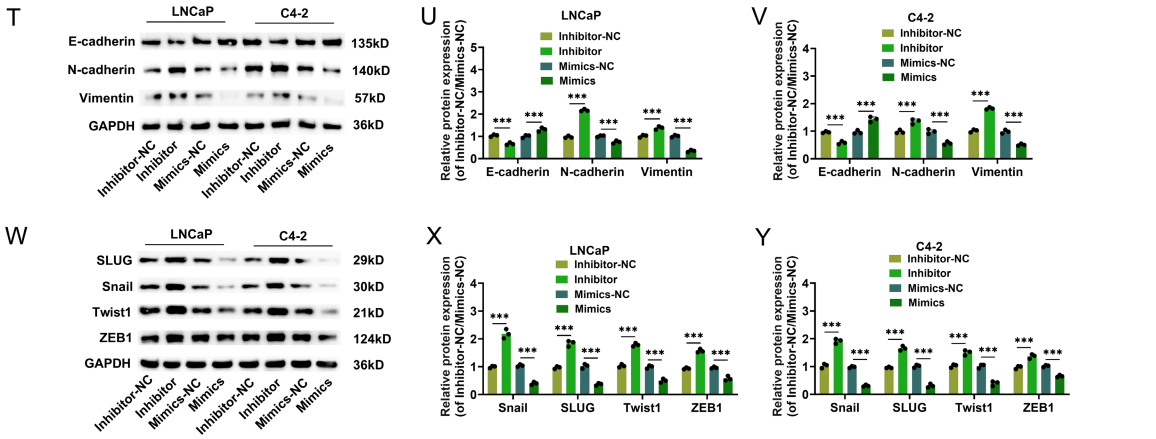

Figure 7. circKLK3-25 can act as a sponge for miR-874-3p, and overexpression of miR-874-3p inhibits the PCa malignant phenotype and EMT. A. Binding site of circKLK3-25 to miR-874-3p was predicted by Circbank. B. qPCR detection of knockdown and overexpression efficiency of miR-874-3p. C, D. Dual-Luciferase reporter assay detected targeted binding of circKLK3-25 to miR-874-3p. E. qRT-PCR to detect changes in miR-874-3p after silencing/overexpression of circKLK3-25. F-H. Western blot detection of p-JNK/JNK, p-ERK/ERK protein expression in tumor tissues. I. Prediction of ERK binding site to miR-874-3p by ENCORI database. J, K. Dual-Luciferase reporter assay detected targeted binding of ERK to miR-874-3p. L, M. EdU staining detected cell proliferation after silencing or overexpression of miR-874-3p (20×, 100 μm). N, O. Scratch-wound assay measured cell migration (10×, 200 μm). P, Q. Transwell assay detected cell invasion (20×, 100 μm). R, S. Flow cytometry to detect apoptosis rate. T-Y. Western blot measured E-cadherin, N-cadherin, Snail, SLUG, Twist1, ZEB1, and Vimentin expression levels in LNCaP and C4-2 cells. n=3. ***P<0.001.

C4-2 cells, in contrast, overexpression of miR-874-3p resulted in a significant decrease in p-JNK/JNK, p-ERK/ERK (**Figure 7F-H**). To further explore the effect of miR-874-3p on the JNK/ERK pathway, we predicted the ERK and miR-874-3p binding sites by ENCORI database (**Figure 7I**). Overexpression of miR-874-3p significantly inhibited the luciferase activity of WT-ERK and had no significant effect on MUT-ERK, suggesting that miR-874-3p binds to ERK (**Figure 7J**, **7K**). Furthermore, overexpression of miR-874-3p significantly reduced the EdU positivity rate of LNCaP and C4-2 cells (**Figure 7L**, **7M**), decreased cell migration and invasion abilities (**Figure 7N-Q**), and increased cell apoptosis rate (**Figure 7R**, **7S**); while silencing miR-874-3p had the opposite effect. Overexpression of miR-874-3p also led to a significant increase in E-cadherin levels, while the expression levels of N-cadherin, Vimentin, Snail, SLUG, Twist1, and ZEB1 were significantly decreased (**Figure 7T-Y**). These results indicate that circKLK3-25 targets and binds to miR-874-3p and acts as its molecular sponge. Overexpression of miR-874-3p can inhibit the JNK/ERK pathway, suppress the malignant biological behavior and EMT process of PCa cells, and promote apoptosis.

Silencing of circKLK3-25 hinders the JNK/ERK signaling pathway and thus tumor growth in vivo

Finally, PCa tumor models were grafted subcutaneously in nude mice to investigate the action of circKLK3-25 in the tumor expansion *in vivo*. Injection of C4-2 cells transfected with sh-circKLK3-25 resulted in a significant decline in circKLK3-25 level in tumor tissues, whereas injection of C4-2 cells transfected with circKLK3-25 caused a significant rise in circKLK3-25 level. It was demonstrated that injection of C4-2 cells transfected with sh-circKLK3-25/circKLK3-25 effectively regulated the level of circKLK3-25 in tumor tissues (**Figure 8A**). The tumor with dampened circKLK3-25, compared with the control group, obtained reduced weight and volume (**Figure 8B-D**). In addition, silencing circKLK3-25 led to a decline in Ki-67 level and a increase in TUNEL positivity, whereas overexpression of circKLK3-25 did the opposite, suggesting that silencing circKLK3-25 inhibited tumor proliferation and promoted apoptosis (**Figure 8E-H**). Immunofluorescence results also showed that silencing circKLK3-25 increased E-cadherin and decreased Vimentin levels, while overex-

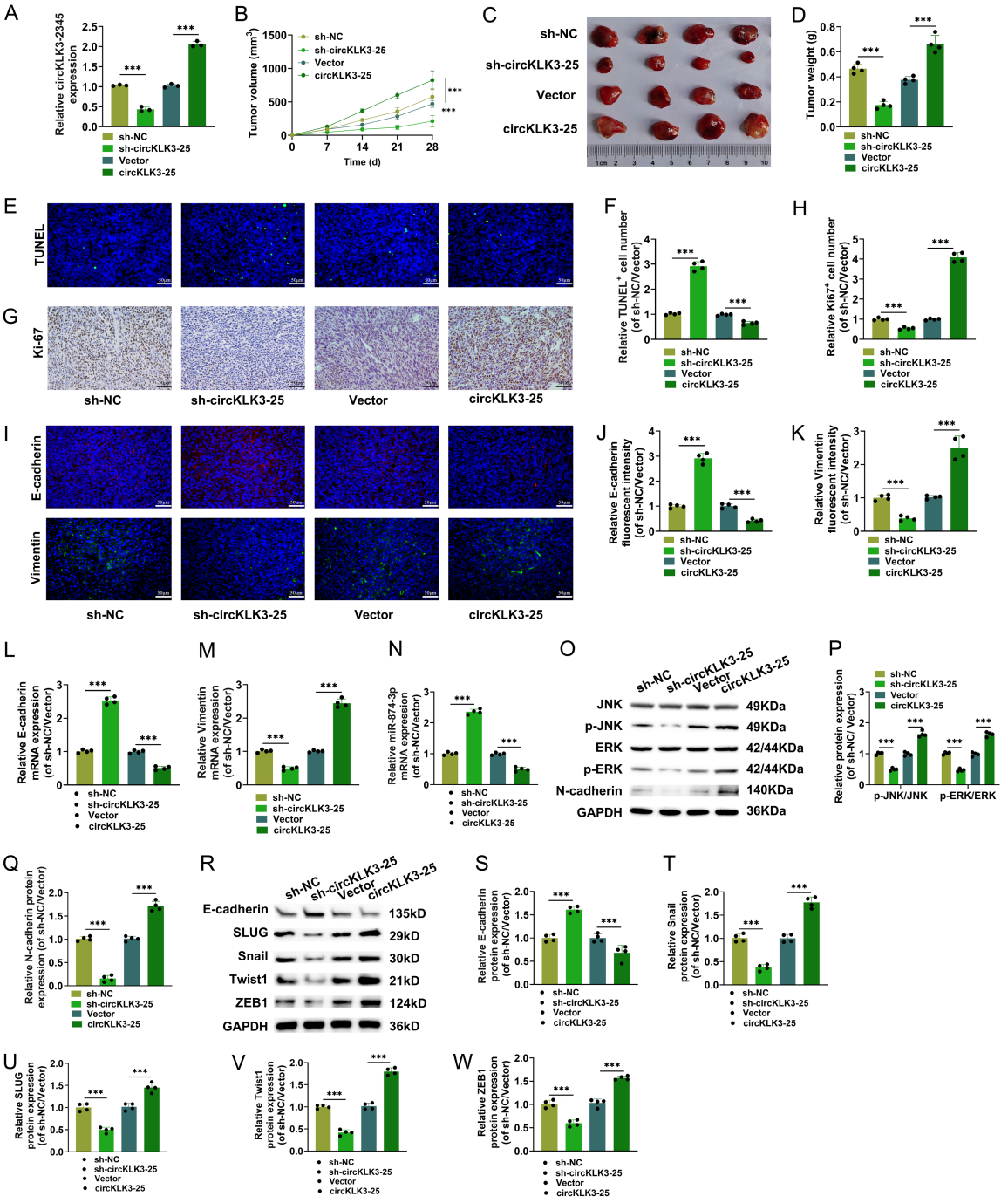

Figure 8. Dampened circKLK3-25's inhibition of tumor expansion in nude mice. A. qRT-PCR assessed circKLK3-25 level in tumor tissues. B-D. The size of subcutaneous tumors in nude mice was measured weekly, the tumors were excised on the 28th d, and photographed and weighed. E, F. The percentage of TUNEL-positive cells in tumor tissues was detected by TUNEL staining (40×, 50 μm). G, H. Immunohistochemistry assessed Ki-67 positivity in tumor tissues (40×, 50 μm). I-K. Immunofluorescence measured E-cadherin and Vimentin levels in tumor tissues (40×, 50 μm). L-N. qRT-PCR detection of E-cadherin, Vimentin, and miR-874-3p expression in tumor tissues. O-W. Western blot detected p-JNK/JNK, p-ERK/ERK, E-cadherin, N-cadherin, Snail, SLUG, Twist1, ZEB1, and Vimentin expression in tumor tissues. n=4. ***P<0.001.

pression of circKLK3-25 did the opposite (**Figure 8I-K**). Silencing circKLK3-25 caused a marked increase in E-cadherin mRNA and a notable decline in Vimentin mRNA level, and

overexpression circKLK3-25 led to the opposite result (**Figure 8L**, **8M**). Not only that, silencing circKLK3-25 upregulated miR-874-3p levels in tumor tissues, whereas overexpression of circKLK3-25 downregulated miR-874-3p (**Figure 8N**). Interestingly, silencing circKLK3-25 caused a significant reduction of p-JNK/JNK, p-ERK/ERK, N-cadherin, Snail, SLUG, Twist1, and ZEB1 levels in tumor tissues and a rise in E-cadherin level, and the opposite was true for overexpression circKLK3-25 (**Figure 8O-W**). These results confirm that silencing circKLK3-25 inhibits JNK/ERK signaling and hinders tumor growth and EMT *in vivo*.

Discussion

As demonstrated by many studies reported recently, circRNAs are vital in controlling the onset and evolution of many malignancies, involving PCa [34], breast cancer [35], gastric cancer [36], and hepatocellular carcinoma [37]. For instance, Ding *et al*. reported that circPDE5A is much down-regulated in PCa tissues and can inhibit PCa cells *in vitro/vivo* from migrating and penetrating; it can also inactivate the MAPK pathway by interfering with the translation of EIF3C, thereby impairing the advancement of PCa [38]. Guo *et al*. discovered that circARHGEF28 is regulated down significantly in tissues and cell lines of PCa, and can block the NF-κB pathway, further preventing PCa cells from multiplying, moving, and penetrating [39]. In the present survey, circKLK3-25 was confirmed existing in PCa cells and its expressions in PCa cell lines were superior to that in RWPE-1 cells.

With a covalently closed circular structure, circRNA has a half-life approximately 2.5 times the corresponding linear RNA and also a higher stability than the latter; circRNA can accumulate in plasma, saliva, and even circulating exosomes, holding a potential to serve as diagnostic, prognostic, and predictive biomarkers [40, 41]. The present survey also demonstrated that circKLK3-25 was insusceptible to RNase R, with a half-life exceeding 48 hours, making it more stable than linear KLK3 mRNA. To discover the specific role of circKLK3-25 in modulating the aggressive evolution of PCa, we had cells LNCaP and C4-2 transfected with circKLK3-25 and sh-circKLK3-25. As an outcome, the PCa cells obtaining excessive circKLK3-25 became strengthened in the abilities to multiply, move, and penetrate, while those obtaining dampened circKLK3-25 showed the contrary trend. EMT, as a complex and important biological process, is characterized by the gradual transformation of epithelial cells into mesenchymal-like cells under the influence of external factors and the loss of their original epithelial cell functions and characteristics [42, 43]. In this process, intercellular adhesion molecules (e.g., E-cadherin) are downregulated, whereas mesenchymal cell markers (e.g., N-cadherin and Vimentin) are upregulated, and the cells exhibit greater migration and proliferation capacity [44]. In this study, overexpression circKLK3-25 promoted the EMT process in PCa cells and tumor tissues, whereas silencing circKLK3-25 did the opposite. This outcome denotes that circKLK3-25 may be an oncogene in PCa cells.

miRNAs are short-chain non-coding RNAs of about 19-24 nucleotides in length, which can regulate the expression of target genes and participate in biological processes such as cell proliferation, differentiation, and migration, and abnormal changes in their expression levels are closely related to the development of various malignant tumors [45, 46]. One of the most important functions of circRNAs is their ability to act as molecular sponges for miRNAs to bind to, attenuating the inhibition of target mRNAs by miRNAs and thus regulating mRNA expression. This mechanism enables circRNAs to regulate miRNAs and thus influence tumor progression [47, 48]. For example, Liu et al. demonstrated that Hsa_circ_0001073 upregulated LIFR expression to inhibit lung cancer progression through sponge adsorption of miR-626 [49]. To elucidate the specific mechanism by which circKLK3-25 promotes PCa progression, we found that with circKLK3-25 can act as a sponge for miR-874-3p through the Circbank database. circKLK3-25 negatively regulates miR-874-3p expression, whereas overexpression of miR-874-3p inhibits the malignant biological behavior and EMT process of PCa cells and promotes apoptosis.

Abnormalities in the MAPK pathway are key factors in carcinogenesis and are associated with multiple aspects of tumors, like cell proliferation, differentiation, angiogenesis, invasion,

and metastasis [50, 51]. As an important component of the MAPK pathway, the JNK/ERK signaling pathway regulates cell cycle, cell proliferation, angiogenesis, apoptosis, etc., and plays an important role in cancer development and progression [52, 53]. It has been shown that overexpression JNK promotes proliferation and invasion in CRPC and that patients with low JNK expression have a higher survival rate [24]. Zhang *et al*. found that inhibition of ERK phosphorylation suppressed EMT in PCa cells [54]. The present survey uncovered that heightening the circKLK3-25 level could drive the phosphorylation of JNK and ERK in PCa cells, while dampening the circKLK3-25 expression could retard it. This result demonstrates the competence of circKLK3-25 to regulate and control the JNK/ERK signal transduction pathway. Alongside this, SP600125 (the JNK inhibitor) and U0126 (the ERK inhibitor) weakened excessive circKLK3-25's action to activate the JNK/ERK pathway, as well as its action to drive cell penetration, movement, and multiplication. This suggests that circKLK3-25 can exert its oncogenic effects by regulating the JNK/ERK signal transduction pathway. In addition, overexpression of miR-874-3p inhibited the JNK/ERK pathway, suggesting that circKLK3-25 may regulate the JNK/ERK pathway by modulating the expression of miR-874-3p and thus the JNK/ERK pathway. Finally, the *in vivo* experiments demonstrated that silencing circKLK3-25 could reduce the tumor weight and volume in nude mice, and also diminish the expression of Ki-67 (a marker of cell proliferation). Importantly, after retarding the circKLK3-25 expression, the phosphorylation of JNK and ERK in tumor tissues became alleviated. This result further verifies that circKLK3-25 boosts cancer evolution by modulating the JNK/ERK signal transduction pathway.

It must be acknowledged that this study also has certain limitations. The signaling pathways involved in PCa progression are highly complex. This study focused solely on the JNK/ERK pathway; future research may explore the regulatory effects of circKLK3-25 on other relevant pathways and the interactions among these pathways. In situ transplantation or tail vein injection metastasis models can be constructed in the future to systematically validate the regulatory role of circKLK3-25 on key phenotypes such as cell invasion and metastasis *in vivo*. In addition, due to the experimental period and funding, the effects of miRNAs and target genes on the PCa malignant phenotype were not explored in depth in this study for the time being.

Conclusion

circKLK3-25 is highly expressed in PCa cells and may be an oncogene in PCa. In terms of the functioning mechanism, circKLK3-25 acts as a sponge for miR-874-3p, promotes PCa cell proliferation, migration and invasion and EMT through activating JNK/ERK signaling pathway. This study unraveled circKLK3-25's crucial effect on the progression of PCa *in vitro/vivo*. The molecules under the regulatory influence of circKLK3-25 are yet to be sought further. To sum up, circKLK3-25 has the potential to be a biomarker for PCa.

Acknowledgements

This study was supported by Zhejiang Provincial Natural Science Foundation of China (Grant No. LBQ20H050001); Zhejiang Medical and Health Science and Technology Project (Grant No. 2019RC110); and Zhejiang Medical and Health Science and Technology Project (Grant No. 2019KY313).

Disclosure of conflict of interest

None.

Abbreviations

PCa, Prostate cancer; EMT, epithelial-mesenchymal transition; CRPC, castration-resistant prostate cancer; ADT, androgen deprivation therapy; circRNA, Circular RNA; KLK3, Kallikrein-related peptidase 3; PSA, prostate-specific antigen; MAPK, mitogen-activated protein kinase; ERK, extracellular-signal-regulated kinase; JNK, c-Jun N-terminal kinase; TUNEL, TdT-mediated dUTP Nick-End Labeling; BSA, bovine serum albumin; CCK-8, Cell Counting Kit-8.

Address correspondence to: Wei Zheng, Zhejiang Provincial People's Hospital (Affiliated People's Hospital), Hangzhou Medical College, No. 158, Shangtang Road, Hangzhou 310000, Zhejiang, China. E-mail: wszw111111@126.com

References

[1] Wang G, Zhao D, Spring DJ and DePinho RA. Genetics and biology of prostate cancer. Genes Dev 2018; 32: 1105-40.

[2] Rebbeck TR. Prostate cancer genetics: variation by race, ethnicity, and geography. Semin Radiat Oncol 2017; 27: 3-10.
[3] Sekhoacha M, Riet K, Motloung P, Gumenku L, Adegoke A and Mashele S. Prostate cancer review: genetics, diagnosis, treatment options, and alternative approaches. Molecules 2022; 27: 5730.
[4] Sung H, Ferlay J, Siegel RL, Laversanne M, Soerjomataram I, Jemal A and Bray F. Global Cancer Statistics 2020: GLOBOCAN Estimates of Incidence and Mortality Worldwide for 36 Cancers in 185 Countries. CA Cancer J Clin 2021; 71: 209-49.
[5] Teo MY, Rathkopf DE and Kantoff P. Treatment of advanced prostate cancer. Annu Rev Med 2019; 70: 479-99.
[6] Evans AJ. Treatment effects in prostate cancer. Mod Pathol 2018; 31: S110-21.
[7] Nguyen-Nielsen M and Borre M. Diagnostic and therapeutic strategies for prostate cancer. Semin Nucl Med 2016; 46: 484-90.
[8] Mansinho A, Macedo D, Fernandes I and Costa L. Castration-resistant prostate cancer: mechanisms, targets and treatment. Adv Exp Med Biol 2018; 1096: 117-33.
[9] Patop IL, Wüst S and Kadener S. Past, present, and future of circRNAs. EMBO J 2019; 38: e100836.
[10] Ragan C, Goodall GJ, Shirokikh NE and Preiss T. Insights into the biogenesis and potential functions of exonic circular RNA. Sci Rep 2019; 9: 2048.
[11] Sadri F and Rezaei Z. Noncoding RNAs: key modulators of the hippo pathway in hepatocellular carcinoma progression. J Can Biomol Therap 2025; 2: 73-88.
[12] Misir S, Wu N and Yang BB. Specific expression and functions of circular RNAs. Cell Death Differ 2022; 29: 481-91.
[13] Huang A, Zheng H, Wu Z, Chen M and Huang Y. Circular RNA-protein interactions: functions, mechanisms, and identification. Theranostics 2020; 10: 3503-17.
[14] Lin Z, Tang X, Wan J, Zhang X, Liu C and Liu T. Functions and mechanisms of circular RNAs in regulating stem cell differentiation. RNA Biol 2021; 18: 2136-49.
[15] Chen LL. The expanding regulatory mechanisms and cellular functions of circular RNAs. Nat Rev Mol Cell Biol 2020; 21: 475-90.
[16] He AT, Liu J, Li F and Yang BB. Targeting circular RNAs as a therapeutic approach: current strategies and challenges. Signal Transduct Target Ther 2021; 6: 185.
[17] Chen L and Shan G. CircRNA in cancer: fundamental mechanism and clinical potential. Cancer Lett 2021; 505: 49-57.
[18] Rodriguez S, Al-Ghamdi OA, Burrows K, Guthrie PA, Lane JA, Davis M, Marsden G, Alharbi KK, Cox A, Hamdy FC, Neal DE, Donovan JL and Day IN. Very low PSA concentrations and deletions of the KLK3 gene. Clin Chem 2013; 59: 234-44.
[19] Moschini M, Carroll PR, Eggener SE, Epstein JI, Graefen M, Montironi R and Parker C. Low-risk prostate cancer: identification, management, and outcomes. Eur Urol 2017; 72: 238-49.
[20] Wu J, Guo S, Wang L and Liao Z. Correlation analysis between CD133, Klk3 and grhl2 expression and tumor characteristics in prostate cancer. Cell Mol Biol (Noisy-Le-Grand) 2022; 67: 68-73.
[21] Ayyıldız SN and Ayyıldız A. PSA, PSA derivatives, proPSA and prostate health index in the diagnosis of prostate cancer. Turk J Urol 2014; 40: 82-8.
[22] Lv C, Fu S, Dong Q, Yu Z, Zhang G, Kong C, Fu C and Zeng Y. PAGE4 promotes prostate cancer cells survive under oxidative stress through modulating MAPK/JNK/ERK pathway. J Exp Clin Cancer Res 2019; 38: 24.
[23] Sugasaki M, Ikeda K, Furukawa A, Watanabe K, Kasuga U, Shimizu K, Takatoya M, Matsumoto C, Miyaura C, Tominari T, Itoh Y, Hirata M and Inada M. Prostate cancer-induced bone formation controlled by bone resorptive inflammatory cytokine IL-1. Biochem Biophys Res Commun 2025; 792: 152966.
[24] Feng Y, Cao H, Wang D, Chen L, Gao R and Sun P. JNK promotes the progression of castration-resistant prostate cancer. Acta Biochim Pol 2023; 70: 817-22.
[25] Wang H, Liang S, Du X, Zhao G, Bai Y, Li J, Xu H, Peng S, Yuan Y and Tang W. RAB26 promotes prostate cancer progression via the MAPK/ERK-TWIST1 signaling axis. Genes Dis 2025; 12: 101689.
[26] Cheng X, Chen M and Liu Z. MicroRNA-294 promotes cell proliferation, migration and invasion in SMMC-7721 hepatoma carcinoma cells by activating the JNK/ERK signaling pathway. Am J Med Sci 2020; 359: 365-71.
[27] Ma Q, Yang F, Huang B, Pan X, Li W, Yu T, Wang X, Ran L, Qian K, Li H, Li H, Liu Y, Liang C, Ren J, Zhang Y, Wang S and Xiao B. CircARID1A binds to IGF2BP3 in gastric cancer and promotes cancer proliferation by forming a circARID1A-IGF2BP3-SLC7A5 RNA-protein ternary complex. J Exp Clin Cancer Res 2022; 41: 251.
[28] Hasimbegovic E, Lukovic D, Kastner N, Hofer BS, Spannbauer A, Traxler D, Mester-Tonczar J, Hamzaraj K, Han E, Riesenhuber M, Maleiner B, Müller-Zlabinger K and Gyöngyösi M. Cardiac circular RNAs CDR1as, Circ-RCAN2, Circ-C12orf29 show cell-specific hypoxia-induced dysregulation and distinct in vitro effects. Int J Mol Sci 2025; 26: 10334.
[29] Luo J, Li Y, Zheng W, Xie N, Shi Y, Long Z, Xie L, Fazli L, Zhang D, Gleave M and Dong X. Charac-

terization of a prostate- and prostate cancer-specific circular RNA encoded by the androgen receptor gene. Mol Ther Nucleic Acids 2019; 18: 916-26.
[30] Jian X, He H, Zhu J, Zhang Q, Zheng Z, Liang X, Chen L, Yang M, Peng K, Zhang Z, Liu T, Ye Y, Jiao H, Wang S, Zhou W, Ding Y and Li T. Hsa_circ_001680 affects the proliferation and migration of CRC and mediates its chemoresistance by regulating BMI1 through miR-340. Mol Cancer 2020; 19: 20.
[31] Zhao B, Yang J, Ran F, Shi Y, Yang L, Duan Y, Shi Z, Li X, Zhang J, Li Z and Wang J. CircBIRC6 affects prostate cancer progression by regulating miR-574-5p and DNAJB1. Cancer Biol Ther 2024; 25: 2399363.
[32] Zhao R, Zhao D, Zhu X, Li F, Xiong P, Li S and Liu J. The influence of miR-3149 on the malignancy progression of gastric cancer by negatively regulating CEACAM5. J Can Biomol Therap 2024; 1: 1-10.
[33] Beeraka NM, Nagalakshmi A, Satyavathi A, Kote DM, Padmanabha RY, Basappa B, Nikolenko VN, Bannimath G, Bulygin KV and Mahesh PA. Ginsenoside Rh4 suppresses notch3 and PI3K/Akt pathway to inhibit growth and metastasis of gastric cancer cells. J Can Biomol Therap 2025; 2: 145-56.
[34] Yu YZ, Lv DJ, Wang C, Song XL, Xie T, Wang T, Li ZM, Guo JD, Fu DJ, Li KJ, Wu DL, Chan FL, Feng NH, Chen ZS and Zhao SC. Hsa_circ_0003258 promotes prostate cancer metastasis by complexing with IGF2BP3 and sponging miR-653-5p. Mol Cancer 2022; 21: 12.
[35] Liu Z, Zhou Y, Liang G, Ling Y, Tan W, Tan L, Andrews R, Zhong W, Zhang X, Song E and Gong C. Circular RNA hsa_circ_001783 regulates breast cancer progression via sponging miR-200c-3p. Cell Death Dis 2019; 10: 55.
[36] Yuan G, Ding W, Sun B, Zhu L, Gao Y and Chen L. Upregulated circRNA_102231 promotes gastric cancer progression and its clinical significance. Bioengineered 2021; 12: 4936-45.
[37] Huang G, Liang M, Liu H, Huang J, Li P, Wang C, Zhang Y, Lin Y and Jiang X. CircRNA hsa_circRNA_104348 promotes hepatocellular carcinoma progression through modulating miR-187-3p/RTKN2 axis and activating Wnt/β-catenin pathway. Cell Death Dis 2020; 11: 1065.
[38] Ding L, Wang R, Zheng Q, Shen D, Wang H, Lu Z, Luo W, Xie H, Ren L, Jiang M, Yu C, Zhou Z, Lin Y, Lu H, Xue D, Su W, Xia L, Neuhaus J, Cheng S and Li G. circPDE5A regulates prostate cancer metastasis via controlling WTAP-dependent N6-methyladenisine methylation of EIF3C mRNA. J Exp Clin Cancer Res 2022; 41: 187.
[39] Guo K, Shi J, Tang Z, Lai C, Liu C, Li K, Li Z and Xu K. Circular RNA circARHGEF28 inhibited the progression of prostate cancer via the miR-671-5p/LGALS3BP/NF-κB axis. Cancer Sci 2023; 114: 2907-19.
[40] Kristensen LS, Jakobsen T, Hager H and Kjems J. The emerging roles of circRNAs in cancer and oncology. Nat Rev Clin Oncol 2022; 19: 188-206.
[41] Liu CX and Chen LL. Circular RNAs: characterization, cellular roles, and applications. Cell 2022; 185: 2016-34.
[42] Manfioletti G and Fedele M. Epithelial-mesenchymal transition (EMT). Int J Mol Sci 2023; 24: 11386.
[43] Papanikolaou S, Vourda A, Syggelos S and Gyftopoulos K. Cell plasticity and prostate cancer: the role of epithelial-mesenchymal transition in tumor progression, invasion, metastasis and cancer therapy resistance. Cancers (Basel) 2021; 13: 2795.
[44] Castellón EA, Indo S and Contreras HR. Cancer stemness/epithelial-mesenchymal transition axis influences metastasis and castration resistance in prostate cancer: potential therapeutic target. Int J Mol Sci 2022; 23: 14917.
[45] Hill M and Tran N. miRNA interplay: mechanisms and consequences in cancer. Dis Model Mech 2021; 14: dmm047662.
[46] Ferragut Cardoso AP, Banerjee M, Nail AN, Lykoudi A and States JC. miRNA dysregulation is an emerging modulator of genomic instability. Semin Cancer Biol 2021; 76: 120-31.
[47] Ma X, Lou C, Pan J, Zhou C, Zhao X, Li N, Tian H and Meng X. The diagnostic potential of a circRNA-miRNA network in non-small cell lung cancer. J Mol Med (Berl) 2023; 101: 671-84.
[48] Nemeth K, Bayraktar R, Ferracin M and Calin GA. Non-coding RNAs in disease: from mechanisms to therapeutics. Nat Rev Genet 2024; 25: 211-32.
[49] Liu Q, Cao G, Wan Y, Xu C, He Y and Li G. Hsa_circ_0001073 targets miR-626/LIFR axis to inhibit lung cancer progression. Environ Toxicol 2021; 36: 1052-60.
[50] Hussain MS, Afzal O, Gupta G, Altamimi ASA, Almalki WH, Alzarea SI, Kazmi I, Fuloria NK, Sekar M, Meenakshi DU, Thangavelu L and Sharma A. Long non-coding RNAs in lung cancer: unraveling the molecular modulators of MAPK signaling. Pathol Res Pract 2023; 249: 154738.
[51] Shorning BY, Dass MS, Smalley MJ and Pearson HB. The PI3K-AKT-mTOR pathway and prostate cancer: at the crossroads of AR, MAPK, and WNT signaling. Int J Mol Sci 2020; 21: 4507.
[52] Abdelrahman KS, Hassan HA, Abdel-Aziz SA, Marzouk AA, Narumi A, Konno H and Abdel-

Aziz M. JNK signaling as a target for anticancer therapy. Pharmacol Rep 2021; 73: 405-34.

[53] Xu F, Xie Q, Li YW, Jing QQ, Liu XJ, Xu YC, Wang X, Liu L, Kim G, Choi Y, Guo Y, Zhang E and Jin CY. Suppression of JNK/ERK dependent autophagy enhances Jaspine B derivative-induced gastric cancer cell death via attenuation of p62/Keap1/Nrf2 pathways. Toxicol Appl Pharmacol 2022; 438: 115908.

[54] Zhang B, Zhang M, Li Q, Yang Y, Shang Z and Luo J. TPX2 mediates prostate cancer epithelial-mesenchymal transition through CDK1 regulated phosphorylation of ERK/GSK3β/SNAIL pathway. Biochem Biophys Res Commun 2021; 546: 1-6.